In-Situ Small-Angle Neutron Scattering from a Block Copolymer Solution under Shear

N. P. Balsara,*,† B. Hammouda,*,‡ P. K. Kesani,† S. V. Jonnalagadda,† and G. C. Straty§

Department of Chemical Engineering, Polytechnic University, Six Metrotech Center, Brooklyn, New York 11201, National Institute of Standards and Technology, Building 235, E151, Gaithersburg, Maryland 20899, and Thermophysics Division, National Institute of Standards and Technology, Boulder, Colorado 80303

Received October 26, 1993; Revised Manuscript Received February 7, 1994®

ABSTRACT: Small-angle neutron scattering profiles from a concentrated (65 wt %) polystyrene–polyisoprene block copolymer solution in dioctyl phthalate under shear were obtained both above and below the quiescent order–disorder transition (ODT). The ordered solution has a lamellar structure under quiescent conditions. The shear-induced structure was inferred from scattering measurements in two planes: the $\mathbf{v}$–$\mathbf{v}\times\nabla v$ plane and the ∇v–$\mathbf{v}\times\nabla v$ plane ($\mathbf{v}$ is the fluid velocity direction and ∇v is the velocity gradient direction). Below the quiescent ODT, oscillatory shear produces lamellae that are aligned along the shearing surface, while steady shear results in a reorientation of the lamellae normals from the $\mathbf{v}$–$\mathbf{v}\times\nabla v$ plane to the ∇v–$\mathbf{v}\times\nabla v$ plane. Above the quiescent ODT, steady shear induces order above a critical shear rate. The resulting scattering anisotropy obtained at different temperatures obeys a universal scaling law, and the critical shear rate increases exponentially with temperature.

Introduction

Rheology, or the relationship between stress and deformation, is a subject of fundamental interest. Rheological relationships are best understood when a model that describes the microscopic effect of the applied stress is established. Microscopic theories based on the de Gennes–Doi–Edwards tube model[1,2] have provided stress–deformation relationships for a variety of homogeneous polymer systems.[3]

Much less is known about the rheological properties of microstructured materials such as block copolymers. The rheological properties of ordered block copolymers are often referred to as "anomalous"[4] because the physical origin of the observed stress–deformation relationship is not fully understood. One of the complexities of such systems is the myriad of possible microscopic responses to applied stress. However, *in-situ scattering* experiments under shear provide avenues for direct experimental observation of the microscopic rearrangement (at the microstructural level, not at the individual chain level).

In this study we focus on systems with a lamellar microstructure. The influence of shear on self-assembled molecular layers such as smectic liquid crystals and block copolymer lamellae has received considerable recent attention.[5-9] Shear modulus measurements are used routinely to track order–disorder transitions in block copolymers.[10] These multilayered materials are also of fundamental importance because they provide models for probing the effect of shear on two-dimensional systems.

The ability of shear to reorient block copolymer layers was demonstrated many years ago by Keller and coworkers.[11] There is now a growing body of evidence indicating that shear fields can induce the formation of ordered layers in systems that would be isotropic under quiescent conditions.[5,7,9] The question of orientation of the layers relative to the velocity ($\mathbf{v}$) and velocity gradient (∇v) directions is an issue of central importance. Isolated rigid layers are expected to orient along streamlines with layer normals oriented in the ∇v direction. However, for interacting fluid layers the answer is not so straightforward and may depend on many factors such as rigidity of the layers, mobility within each layer, initial configuration, and interlayer interactions. These factors may differ from system to system because of differences in molecular architecture, fluctuations, and the concomitant *local* flow fields that must be generated to accommodate the reorientation of the stacks of layers. Indeed experiments on different systems reveal diametrically opposite orientations. Most of the early work on sheared block copolymers suggested that the layer normals orient in the ∇v direction, much like isolated sheets.[11,12] However, some recent studies reveal the possibility of orientation of the layer normals in the vorticity ($\mathbf{v}\times\nabla v$) direction. In-situ small-angle X-ray scattering measurements of Safinya and coworkers showed that normals of shear-induced smectic liquid crystal layers were indeed oriented in the $\mathbf{v}\times\nabla v$ direction.[5] Koppi et al.[7] obtained similar results from block copolymer melts. Such experiments on other structured materials such as colloidal suspensions,[13,14] binary mixtures in the vicinity of the spinodal,[15-17] micellar solutions,[18,19] and cylindrical block copolymers[20] have also been conducted.

We have studied the effect of steady and oscillatory shear on a concentrated block copolymer solution. Under quiescent conditions, the solution exhibits an ordered, lamellar morphology at low temperatures (below 38 °C) and an isotropic, disordered phase at high temperatures (above 38 °C). Experiments were performed in the ordered as well as the disordered state. The structure of the solution under shear was inferred from in-situ small-angle neutron scattering measurements in two planes: the $\mathbf{v}$–$\mathbf{v}\times\nabla v$ plane and the ∇v–$\mathbf{v}\times\nabla v$ plane. The scattering in all three principal directions—$\mathbf{v}$, ∇v, and $\mathbf{v}\times\nabla v$—was thus measured directly. A summary of these results has appeared in a recent paper.[21]

Experimental Section

A nearly monodisperse polystyrene–polyisoprene block copolymer was synthesized by high-vacuum anionic polymerization.

* Authors to whom correspondence should be addressed.
† Polytechnic University.
‡ NIST, Gaithersburg, MD.
§ NIST, Boulder, CO.
® Abstract published in *Advance ACS Abstracts*, March 15, 1994.

0024-9297/94/2227-2566$04.50/0

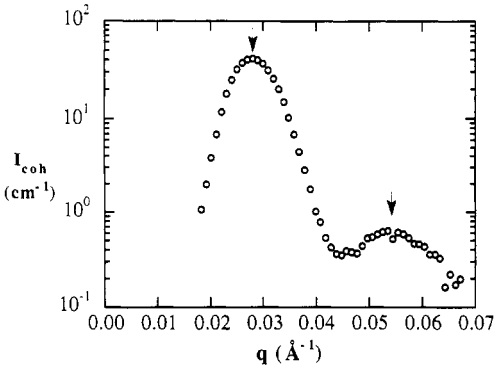

Figure 1. Coherent SANS intensity, I_{coh}, versus scattering vector, q, from pure SI(11-17). The two peaks signify a lamellar structure with a spatial period of 225 Å.

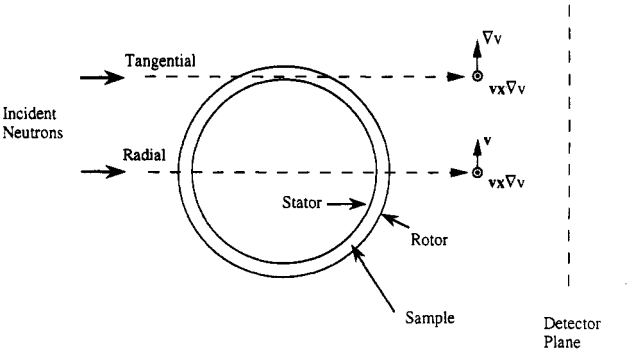

Figure 2. Schematic of the experimental setup. The block copolymer solution was placed between the stator and the rotor. The cell was translated with respect to the incident neutrons so that the beam traveled either radially or tangentially through the shear cell to give the SANS profiles in the $\mathbf{v}$–$\mathbf{vx}\nabla v$ and ∇v–$\mathbf{vx}\nabla v$ planes, respectively.

The polymer will be referred to as SI(11-17); the molecular weights of the polystyrene and polyisoprene blocks were determined to be 1.1×10^4 and 1.7×10^4, respectively, using methods outlined elsewhere.[22] The polydispersity of both blocks was <1.07. Experiments were conducted on a 65 wt % solution of SI(11-17) in bis(2-ethylhexyl) phthalate (dioctyl phthalate, or DOP)—a nonvolatile solvent for both polystyrene and polyisoprene. The DOP, purchased from Aldrich, was treated with Na_2CO_3 and $CaCl_2$ to eliminate impurities, distilled under vacuum (ca. 200 °C, 10^{-4} Torr), and stored in a dry desiccator prior to the experiments. The block copolymer solution was made with benzene as a cosolvent to promote homogenization. The benzene was then removed by evaporation (final stages were carried out in a vacuum oven at 100 °C). The ODT of the solution under quiescent conditions was determined by the birefringence method[23-26] and found to be 38 ± 1 °C.

SANS from pure SI(11-17) was obtained on the 8-m SANS instrument on the NG5 beamline at NIST in Gaithersburg, MD, using procedures described elsewhere.[22] The sample was confined to a 1-mm gap between quartz windows and was made under quiescent conditions. The scattering pattern was azimuthally symmetric, and the circularly averaged SANS data obtained at 50 °C are shown in Figure 1. The primary and secondary peaks corresponding to a lamellar structure with a periodicity of 225 Å are evident. This is expected because the volume fraction of styrene in SI(11-17) is 0.38; lamellar morphology in SI block copolymers is anticipated for polystyrene volume fractions between 0.34 and 0.62.[27] Previous experiments on the concentration dependence of the ODT in SI/DOP solutions[24] indicate that the DOP acts as a plasticizer and is uniformly distributed throughout the sample. Hence one expects ordered SI(11-17)/DOP solutions to also have a lamellar structure.

The SI(11-17)/DOP solution was placed in a quartz Couette shear cell built by G. C. Straty at NIST in Boulder, CO, and described elsewhere.[28] The gap between the outer and inner cylinders was 0.5 mm, which is small compared to the 60-mm diameter of the inner cylinder. The geometry of the shear cell is shown in Figure 2. Shear was imposed on the fluid by rotating the outer cylinder (rotor). The sample temperature was controlled using circulating fluid in the inner cylinder (stator). The alignment of the stator relative to the rotor was adjusted by shearing tetrahydrofuran (THF) at a high shear rate (10 revolutions/s) and finding the position at which the THF–air interface appears motionless and horizontal to the eye. The motion of the rotor was controlled by a computer, which allowed us to impose either steady or oscillatory shear on the solution. All the oscillatory shear measurements were carried out at 200% strain. The time dependence of the displacement of the outer cylinder had a triangular wave form with a fixed frequency of 0.2 Hz.

Before starting a new set of measurements, the effect of shear and thermal history was "erased" by heating the solution under quiescent conditions to a temperature well above 38 °C.

Collimated neutrons with a wavelength (λ) of 5 Å ($\Delta\lambda/\lambda$ = 0.15) were directed through the fluid along either of two paths, as shown in Figure 2. The beam directed along the radial path gives the scattering profile in the $\mathbf{v}$–$\mathbf{vx}\nabla v$ plane, while the tangentially directed beam gives the scattering profile in the ∇v–$\mathbf{vx}\nabla v$ plane. The data were collected in two separate runs on the NG3 beamline at NIST in Gaithersburg, MD, during which most of our measurements were reproduced. Sample-to-detector distances of 5.5 and 6.5 m were used. Two types of apertures were used for the radial measurements: a 13-mm circular aperture, and a 2 mm × 12 mm vertical rectangular slit. Radial scattering patterns from the two apertures were identical, indicating that effects due to beam shape were not significant. The tangential measurements could only be performed with the rectangular slit due to geometric considerations. Of course, due to finite aperture sizes, both the experimentally measured radial and tangential scattering profiles contain some nonradial and nontangential contributions, respectively. Correct alignment of the shear cell relative to the neutron beam was crucial for the tangential measurements. We found that a misalignment of 2 mm in the tangential orientation gave scattering patterns that qualitatively resembled the radial scattering patterns. The SANS profiles were corrected for detector sensitivity and are reported in arbitrary units. We have not attempted to account for the inequality of scattering volumes in the radial and tangential configurations.

Before imposition of shear, the sample was optically clear and devoid of bubbles. However, the start of steady shearing in the ordered state introduced tears near the air–solution interface. These tears soon became elongated bubbles and persisted throughout the measurements. This tearing process appeared to be inevitable under steady shear. This may be due to a flow instability caused by imperfections of the shearing apparatus (concentricity, thermal gradients, etc.). Such phenomena may be further enhanced by the complex rheological properties of ordered block copolymers and may be related to the "slippage" observed in the rheological experiments of Winey et al.[8] The steady-shear flow field was thus only approximately linear in the shear plane. While the motion of these tears was largely unpredictable, the majority of the tears were located above the scattering volume. The experiments reported here were repeated several times, and the measured intensities were reproducible within 5%. In contrast, no tearing was observed during the oscillatory shear experiments.

The sample was first heated to 60 °C, which is well above the birefringence estimate of the ODT, and then cooled to 34 °C. The radial scattering profiles obtained under steady shear with a shear rate $\dot{\gamma} = 2\ s^{-1}$ are shown in Figure 3a, where the intensity is plotted as a function of scattering vectors ($\mathbf{q}$) in the $\mathbf{v}$ and $\mathbf{vx}\nabla v$ directions ($q = |\mathbf{q}| = 4\pi \sin(\theta/2)/\lambda$, where θ is the scattering angle). The scattering pattern obtained after turning off the shear field is shown in Figure 3b. It is evident that the scattering peaks persist, indicating that the anisotropic ordered phase is stable under quiescent conditions. We take this as evidence that the quiescent solution is ordered at 34 °C. The sample was then heated to 43 °C and subjected to the same shear history. The results of these experiments are shown in Figure 4. Careful examination of Figure 4a reveals that the scattering pattern obtained under shear is anisotropic, although the anisotropy in

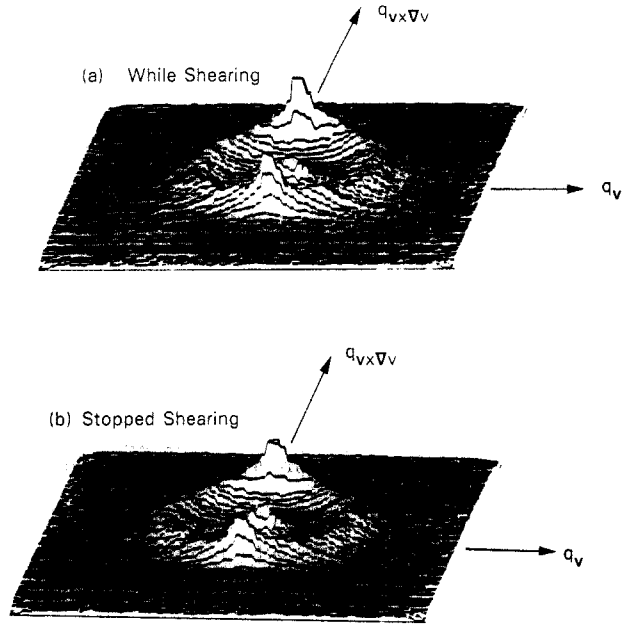

Figure 3. Two-dimensional SANS profiles obtained from the block copolymer solution at 34 °C, which is below the quiescent ODT: (a) while shearing with $\dot{\gamma} = 0.2\ s^{-1}$; (b) after stopping shear.

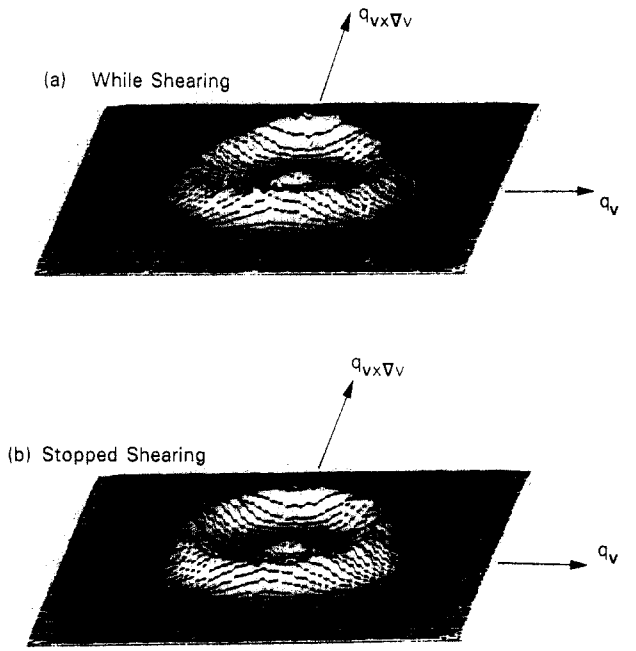

Figure 4. Two-dimensional SANS profiles obtained from the block copolymer solution at 43 °C, which is above the quiescent ODT: (a) while shearing with $\dot{\gamma} = 0.2\ s^{-1}$; (b) after stopping shear.

the intensities in the $v\times\nabla v$ and v directions is no longer as obvious as it was at 34 °C (Figure 3a,b). The scattering pattern obtained after the shear was turned off was symmetric (Figure 4b), indicating that the structure responsible for the SANS anisotropy formed under shear is unstable under quiescent conditions. We thus conclude that the sample is disordered under quiescent conditions at 43 °C and the observed scattering under quiescent conditions is due to disordered fluctuations.[29] Such measurements were repeated at several temperatures and shear rates. The scattering profiles obtained at temperatures greater than or equal to 38 °C were similar to those shown in Figure 4. On the other hand, SANS profiles obtained at temperatures less than or equal to 34 °C were similar to those shown in Figure 3. From these measurements we conclude that the ODT of this solution, under quiescent conditions, occurs at 36 ± 2 °C, which is in reasonable agreement with the ODT determined by birefringence (38 ± 1 °C). Similar SANS determination of the ODT was reported by Koppi et al. in block copolymer melts.[6]

There is, however, some ambiguity in the SANS method of determining the ODT. While the solution is undoubtedly ordered

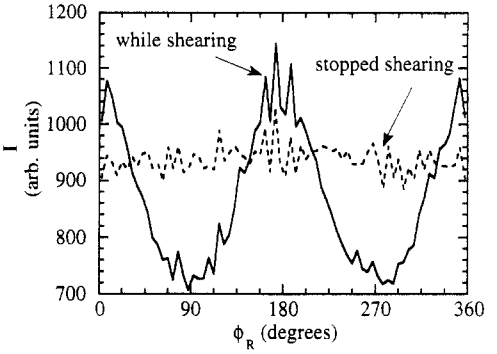

Figure 5. Effect of shear on ring-averaged radial SANS profiles obtained at 43 °C, which is above the quiescent ODT.

at 34 °C, one could argue that the solution is also ordered at 43 °C and that the isotropic scattering pattern obtained after turning the shear field off is due to randomization of the lamellar orientations in the absence of the external field. However, our birefringence result excludes this possibility. It has been proven, both experimentally and theoretically, that ordered block copolymer materials consisting of randomly oriented lamellae are birefringent.[22-26] The lack of birefringence thus proves the absence of randomly oriented lamellae at temperatures above 38 °C.

The data shown in Figures 3 and 4 represent typical scattering profiles obtained in this study. The maximum in the scattering occurred at $q = 0.031 \pm 0.002$ Å^{-1}, regardless of temperature and shear history. In the ordered state, this corresponds to a lamellar spacing of ~200 Å. Most of the scattering from the sample, both above and below the quiescent ODT, is confined to a ring defined by $0.02 < q < 0.04$ Å^{-1}. Plotting the angular dependence of the integrated intensity in this q window is a convenient and compact way of representing the two-dimensional scattering profiles. We define ϕ_R as the azimuthal angle in the radial plane and ϕ_T as the azimuthal angle in the tangential plane, both with reference to the $v\times\nabla v$ direction. The corresponding "ring-averaged" plots of intensity versus ϕ_R obtained from the solution at 43 °C under a shear of $\dot{\gamma} = 2\ s^{-1}$ and after turning off the shear are shown in Figure 5. The anisotropy in the radial scattering profile under shear is more clearly evident in this plot than in the two-dimensional profile (Figure 4a).

Results and Discussion

Effect of Shear at Temperatures below the Quiescent ODT. The sample was disordered by heating to 42 °C (thus erasing the effect of thermal and shear history) and then cooled to 25 °C. This process was carried out in the absence of shear. The radial and tangential scattering profiles obtained at 25 °C are shown in parts a and b of Figure 6, respectively. The radial scattering pattern is nearly isotropic, while the tangential scattering profile has considerable anisotropy. To a good approximation,[30] the measured scattering profiles are only affected by lamellae with normals pointed in the plane normal to the propagation direction. The radial scattering profile thus indicates that lamellae with normals in the v–$v\times\nabla v$ plane have a random orientation distribution. However, the tangential profile indicates that lamellae with normals in the ∇v–$v\times\nabla v$ plane have a strong preference to align along the walls. Thus confining the lamellar sample to a 0.5-mm gap results in preferential alignment of the lamellae even under quiescent conditions. This is surprising because the size of the gap is 4 orders of magnitude greater than the lamellar spacing.

The solution was then sheared at $\dot{\gamma} = 0.2\ s^{-1}$, keeping the sample at 25 °C. Both the tangential and radial profiles (monitored in separate experiments) changed rapidly over the first 30 min or so and then became nearly time independent. The radial and tangential profiles obtained after 30 min of shearing are shown in Figure 7. The radial

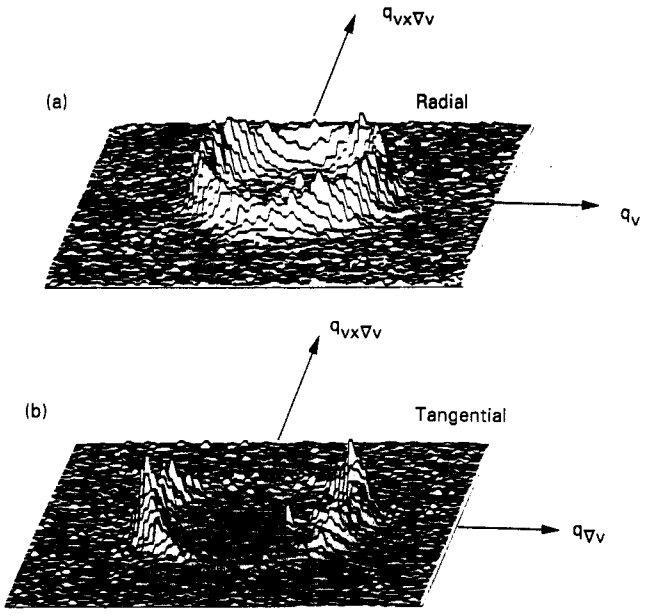

QUIESCENT QUENCH

Figure 6. Two-dimensional SANS patterns obtained from the block copolymer solution after it was quiescently quenched from the disordered state to the ordered state at 25 °C: (a) radial profile; (b) tangential profile.

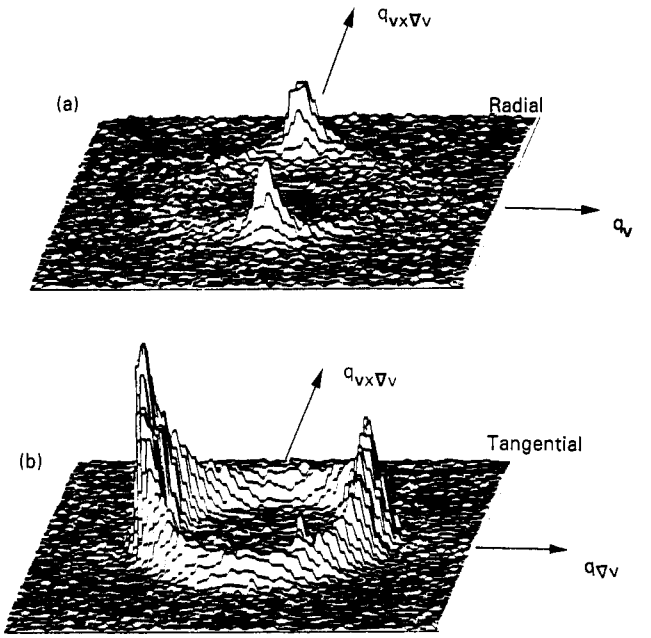

STEADY SHEAR

Figure 7. Two-dimensional SANS patterns obtained from the block copolymer solution under steady shear ($\dot{\gamma}$ = 0.2 s^{-1}) at 25 °C: (a) radial profile; (b) tangential profile.

profile suggests that the layer normals are oriented in the $\mathbf{v}\mathbf{x}\nabla v$ direction while the tangential profile suggests that they are oriented in the ∇v direction. To our knowledge these are the first measurements on block copolymers which demonstrate the possibility of the coexistence of two mutually orthogonal orientations under shear. Note that the radial scattering in directions other than the $\mathbf{v}\mathbf{x}\nabla v$ direction is dramatically reduced after the imposition of steady shear (compare Figures 6a and 7a). Thus layers with normals in the $\mathbf{v}$–$\mathbf{v}\mathbf{x}\nabla v$ plane are unstable to steady shear except for those with normals pointed along the $\mathbf{v}\mathbf{x}\nabla v$ direction. In contrast, there is substantial scattering in all directions in the tangential profile obtained under

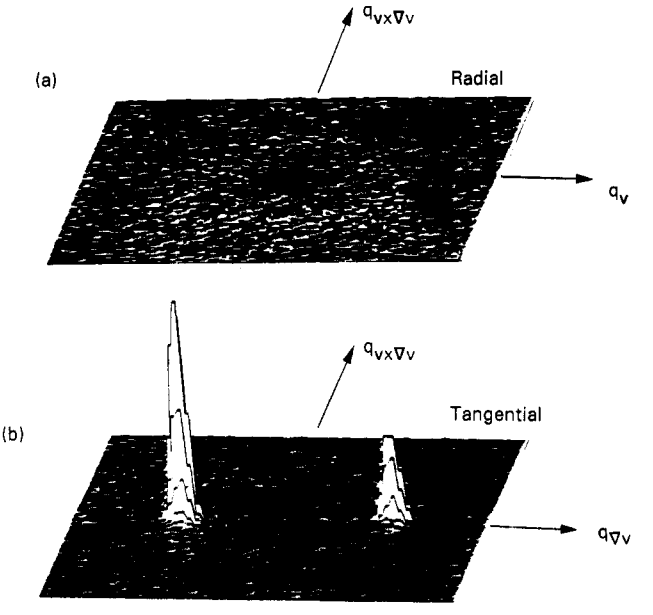

OSCILLATORY SHEAR

Figure 8. Two-dimensional SANS patterns obtained from the block copolymer solution under oscillatory shear (200% strain and ω = 0.2 Hz) at 25 °C: (a) radial profile; (b) tangential profile.

steady shear (Figure 7b). This implies that layers with normals in the ∇v–$\mathbf{v}\mathbf{x}\nabla v$ plane are stable under steady shear. The scattering peak in the ∇v direction indicates a bias for the layer normals to point in the ∇v direction. This bias was, however, already present before the shear field was imposed. Thus the main effect of steady shear is to reorient the layer normals from the $\mathbf{v}$–$\mathbf{v}\mathbf{x}\nabla v$ plane to the $\nabla\mathbf{v}$–$\mathbf{v}\mathbf{x}\nabla v$ plane. Note that steady shear at 34 °C (which is just below the quiescent ODT) produces qualitatively similar results, although the ring in the $\mathbf{v}$–$\mathbf{v}\mathbf{x}\nabla v$ plane (see Figure 3a) indicates that the reorientation occurs to a lesser extent than that at 25 °C. In contrast, Winey et al.[8] observed that the imposition of simple shear on polystyrene–polyisoprene melts results in scattering peaks in the ∇v direction in the ∇v–$\mathbf{v}\mathbf{x}\nabla v$ plane and isotropic scattering in the $\mathbf{v}$–$\mathbf{v}\mathbf{x}\nabla v$ plane.

The solution was then disordered and quenched to 25 °C under quiescent conditions as before. Oscillatory shear (200% strain and ω = 0.2 Hz) was then imposed on the sample. The resulting tangential and radial profiles after 30 min of shearing are shown in Figure 8. It is evident that only layers with normals in the ∇v direction are stable to oscillatory shear. The scattering in all other directions in both the radial and tangential directions is indistinguishable from the background. It is evident that the effect of oscillatory shear is to cause most of the layer normals to point in the ∇v direction. Koppi et al.[6] and Winey et al.[8] observed the same phenomenon in block copolymer melts sheared at low frequency.

In Figure 9a we show the development of alignment after imposition of oscillatory shear where the ring-averaged tangential scattering profiles are shown as a function of time. It is evident that most of the reorientation of lamellae occurs in ~30 min. The oscillatory shear field was then turned off and the sample was subjected to steady shear with $\dot{\gamma}$ = 0.2 s^{-1}. The effect of changing shear fields was monitored by measuring the radial scattering profiles. In Figure 9b we show the time dependence of the ring-averaged scattering profiles. Initially the scattered intensity is low and independent of ϕ_R due to alignment of the lamellae parallel to the cell walls. However, the steady

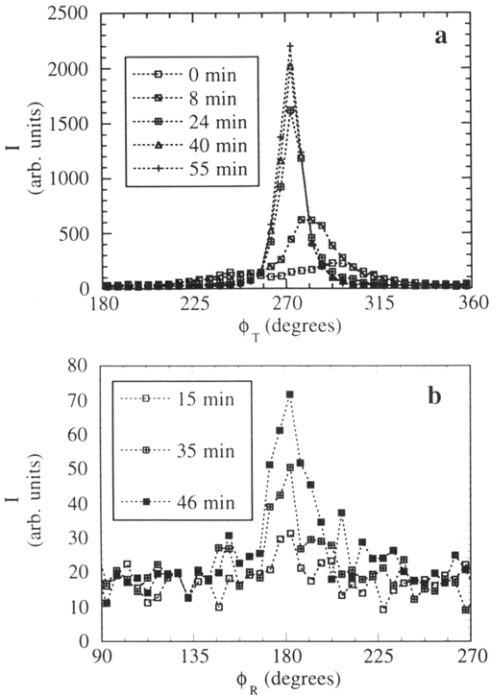

Figure 9. (a, Top) Ring-averaged tangential scattering versus azimuthal angle, ϕ_T, as a function of time after imposing oscillatory shear at $t = 0$ on a quiescently quenched solution. The increasing peak intensity at $\phi_T = 270$ °C indicates a gradual reorientation of the lamellae so that their normals point in the ∇v direction. (b, Bottom) Ring-averaged radial scattering versus azimuthal angle, ϕ_R, as a function of time after switching from oscillatory to steady shear at $t = 0$. The development of the peak at $\phi_R = 180°$ indicates the reappearance of lamellae with normals in the $\mathbf{vx}\nabla v$ direction.

shear field produces scattering maxima at $\phi_R = 0$ and 180°, indicating the reappearance of layers with normals in the $\mathbf{vx}\nabla v$ direction. The radial and tangential profiles obtained after an hour of steady shear were identical to those shown in Figure 7. Switching the shear field back from steady to oscillatory produced the expected result, namely, well-ordered lamellae with normals in the ∇v direction only. We also performed experiments wherein the sample was heated well above the ODT and subjected to steady shear while it was cooled from the disordered to the ordered state. Again, the scattering profiles were similar to those shown in Figure 7. We thus conclude that steady shear produces lamellae with normals in both the $\mathbf{vx}\nabla v$ and ∇v directions, regardless of their initial orientation. The tendency of steady shear to destroy orientation created by oscillatory shear was also observed in block copolymer melts by Winey et al.[8] Similarly, oscillatory shear produces lamellae with layer normals in the ∇v direction only, regardless of their initial orientation.

We propose a simple physical picture that is consistent with our scattering data. Quiescently quenched, lamellar block copolymer materials are composed of randomly oriented layers. Coherent order is restricted to micron-sized regions called "grains".[25,26,31] Recent studies of lamellar block copolymers indicate that there is a preference for continuity of the lamellar microphases across defects.[31] Thus, the unsheared, ordered material may be described as a dense collection of "crumpled sheets" (see Figure 1 in ref 31). The proposed effect of shearing such a crumpled sheet is pictorially depicted in Figure 10. The imposition of steady shear stretches the sheet in the velocity direction (**v**). This smoothens the crumples in the **v** direction but not in the direction perpendicular to it, i.e., in the $\mathbf{vx}\nabla v$ direction. Steady shear thus produces

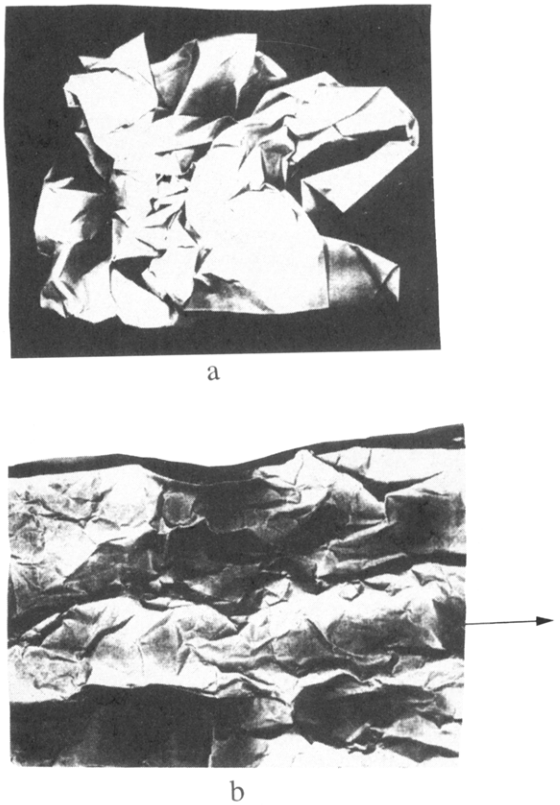

Figure 10. Pictorial representation of the effect of simple shear on quiescently quenched lamellae. (a) Before shearing, the lamellae are randomly crumpled. (b) Upon shearing (the direction of the arrow represents the velocity direction), the lamellae stretch in the velocity direction, resulting in the preferential annihilation of the crumples in this direction. Notice that most of the crumples in the stretched sheet lie in the direction of the arrow. The figure is a photocopy of a crumpled piece of paper (a) which was then stretched out by pulling along the direction of the arrow (b).

sheets that are, on average, crumpled in the $\mathbf{vx}\nabla v$ direction but smooth in the **v** direction with normals in the ∇v direction. The scattering peaks in the tangential profile (see Figure 8b) are due to alignment of the lamellae while the peaks in the radial profile (Figure 8a) and the isotropic ring at the base of the peaks in the tangential profile (see Figure 8b) are attributed to unidirectional crumples or ripples that run along the **v** direction. On the other hand, oscillatory shear produces much more ordering than steady shear with lamellae parallel to the shear cell walls and no evidence of ripples in either the **v** or the $\mathbf{vx}\nabla v$ direction. This effect may be perceived as an "ironing out" of crumples along both directions. We do not imply that oscillatory shear has produced "perfect" alignment of the lamellae. We only claim that the ripples or other defects that may persist under oscillatory shear are much fewer in number than those obtained under simple shear and are within instrumental resolution.

Scattering profiles in the three principal directions can be unambiguously interpreted if the structure orients completely in one of these directions. For the case of the oscillatory shear experiments, we could thus identify the orientation of the lamellae because scattering was only observed along the ∇v direction and the scattering in all other accessible directions was nearly zero (Figure 7). However, this was not the case with the profiles obtained under steady shear, where orientations in the nonprincipal directions were clearly evident in the tangential profiles. In such cases, the limited directions available to us are not enough to unambiguously identify the structure. Many

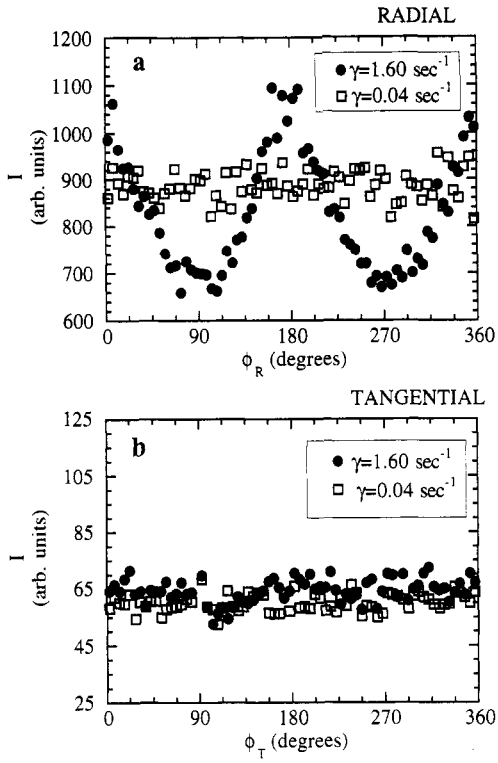

Figure 11. Effect of steady shear on SANS profiles at 43 °C, which is above the quiescent ODT: (a, top) typical ring-averaged radial scattering profiles at low and high shear rates; (b, bottom) typical ring-averaged tangential scattering profiles at low and high shear rates.

other structures (besides crumpled lamellae) may be consistent with the observed scattering patterns.

It is perhaps appropriate to mention that all the SANS data obtained from the SI(11–17)/DOP solution below the quiescent ODT showed a scattering maximum at $q \approx 0.031$ Å^{-1} only; higher order peaks were not observed. This is typical of systems near the ODT. The fact that the location of this maximum is very close to the observed maximum in the scattering from pure SI(11–17)—in which case the lamellar structure could be unambiguously identified due to the presence of the higher order peaks (see Figure 1)—and the fact that the structure under oscillatory shear was definitely lamellar, however, strongly suggest that the structure under quiescent conditions and under steady shear is also lamellar. In addition, the scattering profiles obtained upon shearing below the quiescent ODT persisted after the shearing was stopped (see Figure 3), indicating that the effect of shear was mainly to reorient the existing lamellar structure. If the quiescent and shear-induced structures were different, then one might expect a change in the scattering after turning the shear off. Such effects were only observed above the quiescent ODT and are discussed in the next section.

Effect of Shear at Temperatures above the Quiescent ODT. Most of the experiments above the quiescent ODT were conducted under steady shear. The effect of steady shear on the scattering profiles from the SI(11–17)/DOP solution at 46 °C (which is 8 °C above the quiescent ODT) is shown in Figure 11. The ring-averaged scattered intensity obtained in the radial configuration is plotted as a function ϕ_R in Figure 11a. It is evident that the scattering pattern is isotropic at the low shear rate ($\dot{\gamma}$ = 0.04 s^{-1}) but anisotropic at the high shear rate ($\dot{\gamma}$ = 1.6 s^{-1}). On the other hand, the ring-averaged tangential scattering profiles were found to be isotropic at all shear rates. The ring-averaged scattered intensity for $\dot{\gamma}$ = 0.04 s^{-1} and $\dot{\gamma}$ = 1.6 s^{-1} at 46 °C are shown in Figure 11b; the

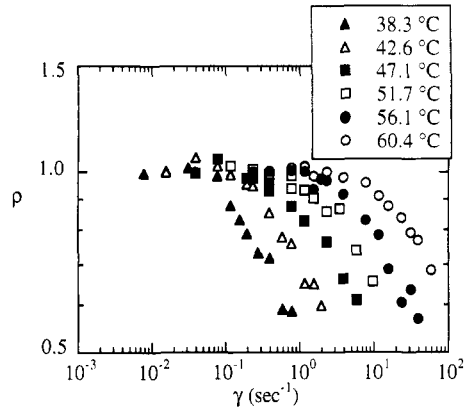

Figure 12. Dependence of the peak anisotropy in the radial scattering profiles, ρ, on shear rate, $\dot{\gamma}$, obtained at different temperatures above the quiescent ODT.

two-dimensional SANS patterns obtained at both shear rates were similar to those shown in Figure 4b. The anisotropy in the radial profiles at high shear rates suggests a restructuring of the SI(11–17)/DOP solution. However, the nature of the formed structure is not clear. The radial profiles suggest that the shear-induced structure may be lamellar, with a bias for layer normals to orient in the $\mathbf{v}\times\nabla v$ direction, as suggested by Cates and Milner.[9] However, the isotropic tangential profiles do not support such an assignment. One possibility is that the shear-induced layers are rectangular with the long sides parallel to $\mathbf{v}$ and the short sides oriented isotropically in the ∇v–$\mathbf{v}\times\nabla v$ plane; i.e., the structure is coherent in the $\mathbf{v}$ direction but not in the ∇v direction. Other structures such as rolled lamellae and cylinders are also consistent with the observed scattering.

Scattering in the radial and tangential geometries of the SI(11–17)/DOP solution was measured at temperatures ranging from 38 to 60 °C. The observed patterns were qualitatively similar to those reported above at 46 °C, i.e., isotropic radial patterns at low shear rates, anisotropic radial scattering patterns at high shear rates, and isotropic tangential patterns at all shear rates. The radial scattering anisotropy at a given temperature and shear rate is quantified by calculating a peak anisotropy ratio, ρ, defined as the ratio of the peak scattered intensity in the $\mathbf{v}\times\nabla v$ direction (ϕ_R = 90, 270°) to that in the $\mathbf{v}$ direction (ϕ_R = 0, 180°). In Figure 12 we plot ρ versus $\dot{\gamma}$ at different temperatures. The scattering anisotropy at a given shear rate and temperature (above the quiescent ODT) was independent of the shear and thermal history of the sample. At high shear rates these data obey the following power law:

$$\rho \sim \dot{\gamma}^{-\beta} \tag{1}$$

where $\beta = 0.19 \pm 0.03$ (based on a 95% confidence interval).

The high shear rate data at each temperature (with $\rho < 0.95$) were fit to power laws and extrapolated to low shear rates. The x coordinate of the point at which these extrapolations intersect the ρ = 1 line is defined as the critical shear rate, $\dot{\gamma}_c$, which may be interpreted as the onset point of the high shear rate structure. In Figure 13 we show that the critical shear rate increases exponentially with temperature. In Figure 14 we plot ρ versus $\dot{\gamma}/\dot{\gamma}_c$. It is evident that all the data fall on a master curve, demonstrating the universal nature of the shear-induced structure in these solutions.

Cates and Milner proposed a theory predicting the possibility of obtaining shear-induced order in block copolymer melts at temperatures above the quiescent

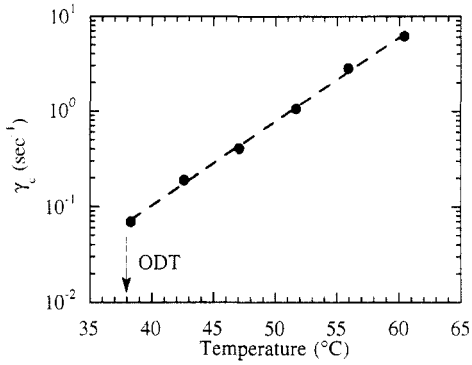

Figure 13. Dependence of the critical shear rate, $\dot{\gamma}_c$, signifying the onset of shear-induced order, on temperature.

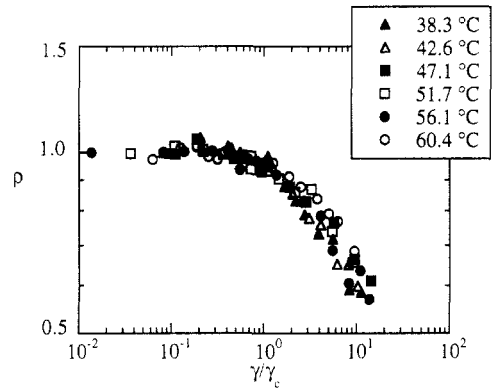

Figure 14. Master curve for the dependence of peak anisotropy in the radial scattering profiles, ρ, versus scaled shear rate, $\dot{\gamma}/\dot{\gamma}_c$, for all temperatures.

ODT.[9] They predicted that the lamellar normals would be oriented in the $\mathbf{v}\mathbf{x}\nabla v$ direction. In-situ SANS experiments on polyolefin diblock copolymers under shear conducted by Koppi et al. were in agreement with these predictions.[7] They measured the SANS intensity in the $\mathbf{v}$–$\mathbf{v}\mathbf{x}\nabla v$ plane and found shear caused the formation of well-defined peaks in the $\mathbf{v}\mathbf{x}\nabla v$ direction above the quiescent ODT. By comparison, the peaks in the $\mathbf{v}$–$\mathbf{v}\mathbf{x}\nabla v$ plane obtained by us at high shear rates (e.g., Figure 11a) are much broader than the peaks obtained by Koppi et al.,[7] indicating a poorly defined structure. Perhaps the structure observed by us represents the initial stages of shear-induced spinodal decomposition. This is further supported by the fact that our measurements showed no evidence of hysteresis; i.e., the value of ρ at a given temperature and shear rate was independent of shear and temperature history. In contrast, Koppi et al. observed significant hysteresis.[7] It is expected that systems in the early stages of spinodal decomposition will exhibit reversibility, while those in the advanced stages of spinodal decomposition will exhibit hysteresis. We also note that Cates and Milner predict a weakening of the shear-induced ODT as temperature (i.e., shear rate) is increased. In contrast, the collapse of the data in Figure 14 suggests a nonweakening of the shear-induced transition in SI(11–17)/DOP solutions in the accessible temperature window.

In Figure 15 we demonstrate the effect of oscillatory shear on the SI(11–17)/DOP solution above the quiescent ODT. The peaks in the tangential profile and the isotropic radial profiles indicate layer formation under shear with preferential alignment along the walls of the shear cell. This is identical to the alignment observed under oscillatory shear below the quiescent ODT. All previous studies of shear-induced order above the quiescent ODT[5,7] have shown that the layer normals are aligned in the $\mathbf{v}\mathbf{x}\nabla v$ direction. Such an orientation has been attributed to

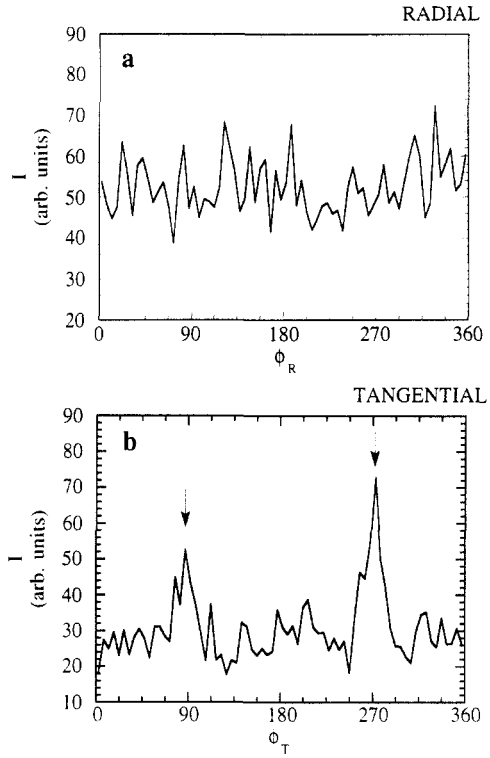

Figure 15. Effect of oscillatory shear on ring-averaged SANS profiles at 41 °C, which is above the quiescent ODT, showing the formation of shear-induced lamellae with normals in the ∇v direction: (a, top) radial profile, (b, bottom) tangential profile.

coupling between concentration fluctuations and the shear field.[9] Our results indicate that the $\mathbf{v}\mathbf{x}\nabla v$ alignment obtained by previous workers above the quiescent ODT[5,7] is not universal to layered systems, and other orientations are possible. This also suggests that order formation above the quiescent ODT may be driven by more than one mechanism. Perhaps there is a competition between fluctuation-driven order that induces layer normals to orient in the $\mathbf{v}\mathbf{x}\nabla v$ direction and the tendency of the viscous torque to align the layer normals in the ∇v direction. The dominant orientation may differ from one system to another due to fundamental differences in the physical nature of the layers. For instance, the molecules comprising liquid crystalline layers[5] can rotate freely about their axis in response to the imposed torque, while such motion is essentially forbidden in block copolymer layers. It is important to emphasize that the oscillatory shear experiments above the quiescent ODT are limited to one temperature and a fixed frequency (0.2 Hz) and strain (200%).

Concluding Remarks

We have performed in-situ SANS measurements on a concentrated solution of a polystyrene–polyisoprene diblock copolymer in DOP under shear. Our results illustrate the importance of measuring SANS profiles in both the radial and tangential directions. The radial profiles alone would have led to incorrect conclusions. We found many surprising results that cannot be explained on the basis of current understanding.

Quiescent quenches from the disordered to the ordered state always resulted in anisotropic lamellar orientation, with preferential alignment along the walls of the shear cell. In these experiments, lamellae with a spacing of 200 Å were confined to a 0.5-mm gap. Certainly, the effect of a finite container size should disappear for large enough containers. The fact that 0.5 mm is not large enough was unexpected.

We found qualitative differences between steady and oscillatory shear. The principal effect of steady shear on quiescently quenched material was to reorient layer normals from the $\mathbf{v}-\mathbf{v}\mathbf{x}\nabla v$ plane to the $\nabla\mathbf{v}-\mathbf{v}\mathbf{x}\nabla v$ plane. The scattering data are consistent with the notion that a solution under steady shear is composed of rippled sheets that lie parallel to the shearing surface. On the other hand, oscillatory shear below the quiescent ODT reorients all lamellae and forces them to lie parallel to the wall with no evidence of ripples.

Most of our experiments above the quiescent ODT were done under steady shear. Above a critical shear rate, which increases exponentially with temperature, we find anisotropic radial scattering patterns indicative of shear-induced structure formation. In contrast, oscillatory shear above the quiescent ODT produced lamellae parallel to the wall, giving isotropic radial patterns and anisotropic tangential patterns.

Albalak and Thomas have recently reported a new process called roll-casting in which a flowing block copolymer solution is devolatilized to give macroscopic block copolymer samples with aligned microstructure.[32] The flow field in these experiments was generated by two corotating eccentric cylinders which produce a combination of an oscillating elongational flow and a steady shear flow. The resulting orientation obtained by Albalak and Thomas was identical to that obtained by us under oscillatory shear. Our experiments suggest that steady shear alone is not sufficient to orient solvated block copolymer lamellae. This suggests that the imposition of the oscillating elongational flow may be crucial to the success of the roll-casting method, ironing out the unidirectional crumples that would otherwise have formed under steady shear alone.

Perhaps more solution-based fabrication processes will emerge as we begin to understand the effects of shear on block copolymer solutions.

Acknowledgment. N.P.B., P.K.K., and S.V.J. acknowledge the donors of the Petroleum Research Fund, administered by the American Chemical Society, the Exxon Education Foundation, and an NIST contract[33] for partial financial support. The work of G.C.S. was supported in part by grants from the Division of Chemical Sciences, Office of Basic Energy Sciences, Office of Energy Research, and the U.S. Department of Energy. The SANS instrument is supported by the NSF under agreement No. DMR-9122444. Helpful discussions with Charles Han and Sanjay Patel are gratefully acknowledged.

References and Notes

(1) de Gennes, P.-G. *J. Chem. Phys.* **1971**, *55*, 572.
(2) Doi, M.; Edwards, S. F. *The Theory of Polymer Dynamics*; Oxford University Press: Oxford, 1986.
(3) Graessley, W. W. In *Physical Properties of Polymers*, 2nd ed.; American Chemical Society: Washington, DC, 1993; Chapter 3 and references therein.
(4) Kawasaki, K.; Onuki, A. *Phys. Rev. A* **1990**, *42*, 3664.
(5) Safinya, C. R.; Sirota, E. B.; Plano, R. J. *Phys. Rev. Lett.* **1991**, *66*, 1986.
(6) Koppi, K. A.; Tirrell, M.; Bates, F. S.; Almdal, K.; Colby, R. H. *J. Phys. (Fr.)* **1992**, *2*, 1941.
(7) Koppi, K. A.; Tirrell, M.; Bates, F. S. *Phys. Rev. Lett.* **1993**, *70*, 1449.
(8) Winey, K. I.; Patel, S. S.; Larson, R. G.; Watanabe, H. *Macromolecules* **1993**, *26*, 2542.
(9) Cates, M. E.; Milner, S. T. *Phys. Rev. Lett.* **1989**, *62*, 1856.
(10) Chung, C. I.; Gale, J. C. *J. Polym. Sci., Polym. Phys. Ed.* **1976**, *14*, 1149.
(11) Folkes, M. J.; Keller, A. *J. Polym. Sci., Polym. Phys. Ed.* **1976**, *14*, 833.
(12) Hadziioannou, G.; Skoulios, A. *Macromolecules* **1982**, *15*, 258.
(13) Clark, N. A.; Ackerson, B. J. *Phys. Rev. Lett.* **1980**, *44*, 1005.
(14) Chen, L. B.; Zukoski, C. F.; Ackerson, B. J.; Hanley, H. M. H.; Straty, G. C.; Barker, J.; Glinka, C. J. *Phys. Rev. Lett.* **1992**, *69*, 688.
(15) Beysens, D.; Gbadamassi, M.; Boyer, L. *Phys. Rev. Lett.* **1979**, *43*, 1253.
(16) Wu, X. L.; Pine, D. J.; Dixon, P. K. *Phys. Rev. Lett.* **1991**, *66*, 2408.
(17) Hobbie, E. K.; Hair, D. W.; Nakatani, A. I.; Han, C. C. *Phys. Rev. Lett.* **1992**, *69*, 1951.
(18) Kalus, J.; Hoffman, H. *J. Chem. Phys.* **1987**, *87*, 714.
(19) Fetters, L. J.; et al., to be published.
(20) Morrison, F. A.; Mays, J. W.; Muthukumar, M.; Nakatani, A. I.; Han, C. C. *Macromolecules* **1993**, *26*, 5271.
(21) Balsara, N. P.; Hammouda, B. *Phys. Rev. Lett.* **1994**, *72*, 360.
(22) Balsara, N. P.; Lin, C. C.; Dai, H. J.; Krishnamoorti, R. *Macromolecules*, to appear.
(23) Amundson, K. R.; Helfand, E.; Patel, S. S.; Quan, X.; Smith, S. S. *Macromolecules* **1992**, *25*, 1953.
(24) Balsara, N. P.; Perahia, D.; Safinya, C. R.; Tirrell, M.; Lodge, T. P. *Macromolecules* **1992**, *25*, 3896.
(25) Balsara, N. P.; Garetz, B. A.; Dai, H. J. *Macromolecules* **1992**, *25*, 6072.
(26) Garetz, B. A.; Newstein, M. C.; Dai, H. J.; Jonnalagadda, S. V.; Balsara, N. P. *Macromolecules* **1993**, *26*, 3151.
(27) Bates, F. S.; Fredrickson, G. H. *Annu. Rev. Phys. Chem.* **1990**, *41*, 525.
(28) Straty, G. C. *NIST J. Res.* **1989**, *94*, 259.
(29) Leibler, L. *Macromolecules* **1980**, *13*, 1602.
(30) Glatter, O.; Kratky, O. *Small Angle X-ray Scattering*; Academic Press: New York, 1982.
(31) Gido, S. P.; Gunther, J.; Thomas, E. L.; Hoffman, D. *Macromolecules* **1993**, *26*, 4506.
(32) Albalak, R. J.; Thomas, E. L. *J. Polym. Sci., Polym. Phys. Ed.* **1993**, *31*, 37.
(33) Certain equipment and instruments or materials are identified in this paper to adequately specify the experimental details. Such identification does not imply recommendation by the National Institute of Standards and Technology nor does it imply the materials are necessarily the best available for the purpose.